

ORIGINAL ARTICLE



Experimental Study on Steel Slit and Shear Panel for Seismic Resistance

Ferit Gashi¹, Franco Bontempi¹, Francesco Petrini¹

Correspondence

Prof.Dr.Franco Bontempi
Sapienza University of Rome,
Via Eudossiana 18,00184 Rome,
Department of Structural and Geotechnical
Engineering.
Email: Franco.bontempi@Unroma1.it

Affiliations

¹ Sapienza University of Rome, Rome,Italy

Abstract

This paper summarizes the experimental campaign carried out for the development of new steel energy dissipative devices named Slit Dampers (SDs) designed for earthquake protection of structures. A total of eighty-two steel shear plates with different openings and thicknesses are tested to investigate their behaviour under cyclic pseudo-static loading. Eight types of steel shear plates are studied, including the SD with narrow slits that divide the plate into rectangular links, and the butterfly fuse with a diamond-shaped opening that creates butterfly shape links in the plate. Other varying test parameters are loading rate, material strength, and the number of in-parallel damper elements. It is expected that the proposed model can be successfully used to predict the behaviour of dampers in real-world applications.

Keywords:

Experimental study, Slit damper, ductility, energy dissipation, passive control

1 Introduction

- Passive control structural systems with seismic dampers have achieved significant progress in recent decades.
- During a major earthquake, a large amount of energy is being pumped into the building. The way in which this energy consumed in a structure determines the level of damage. If this energy can be controlled and distributed independently of structural components, seismic performance and the response of the structure will be significantly improved.
- This can be achieved using the passive control system of structures. Structural control systems can be divided into three classes: Passive, active, and semi-active. Passive control systems are structures equipped with devices for energy distribution that do not require an external power source for vibration response while active or semi-active control systems are the external source of energy for the operation of actuators which supply the control forces in the structure.
- This paper investigates the use of the slit and honeycomb type steel plates as the energy dissipation device for seismic application as shown in Fig.1. The hysteretic behaviour and energy dissipation capacity is evaluated via component tests under cyclic loads. Finally, seismic performance test on large-scale structure was conducted to further verify the feasibility and effectiveness of the new seismic damper.

2 Research Objectives

Numerous studies have been reported on the design of steel plates with cracks or openings. Previous research has shown steel plates with slit or openings can potentially provide a simple and cost-effective solution. Three types of fuse geometries are chosen in this study to be further investigated, including plates with straight slits referred to as the slit fuses and plates with butterfly. Where thin fuses are defined as having width to thickness $L/t = 200/20 = 10, 20, 25, 50$. In this study, eight steel damper specimens were made from mild steel plate and using cutting waterjet with specific geometry (Figure 2). The tests were performed in the Structural Laboratory of Sapienza University of Rome. The aim of the test is to determine which among the two proposed dampers has large energy absorption capabilities, stable hysteresis loop, and adequate stiffness.

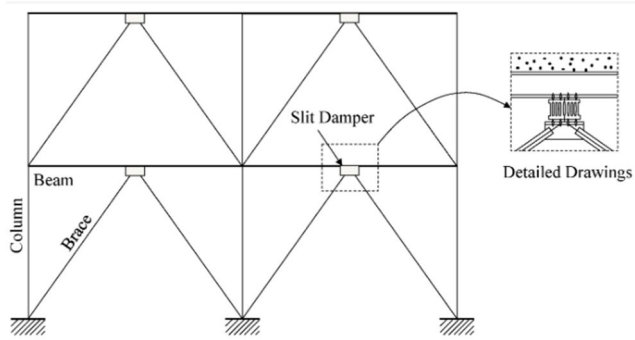
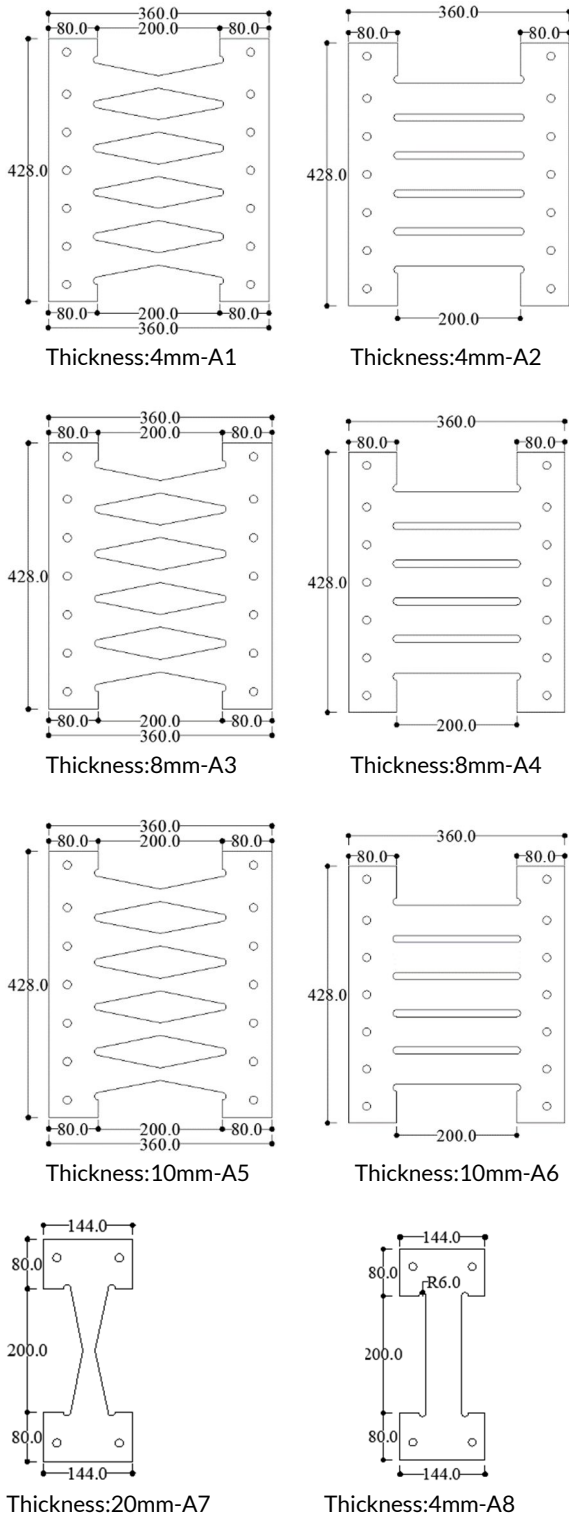


Fig.1. Installation of the slit damper Device in the concentrically braced frame, link: <https://www.mdpi.com/2076-3417/5/3/187/htm>



Fig.1 In Execution!! Rehabilitation Tirana Hospital (Autor:F.Gashi , prof.Markel Baballeku) ecc.



Specimens	Material	Thickness mm	Width b	Height	Loading Amplitude
Specimen A1	S-235	4mm	60	200	Increasing-AISC
Specimen A2	S-235	4mm	50	200	Increasing-AISC
Specimen A3	S-355	8mm	60	200	Increasing-AISC
Specimen A4	S-355	8mm	50	200	Increasing-AISC
Specimen A5	S-275	10mm	60	200	Increasing-AISC
Specimen A7	S-275	10mm	50	200	Increasing-AISC
Specimen A8	S-235	20mm	60	200	Increasing-AISC
Specimen A8	S-235	20mm	60	200	Increasing-AISC

3.0 Experimental Program

Various types of cyclic tests were performed using a 500 kN hydraulic servo fatigue test machine, The MTS controller received commands from the control computer, and sent signals to the actuator, it also received back displacement and force readings for the actuator, Time history. A total of eight samples with specific geometry were cut using the water jet machine to take shape and precise dimensions. The specimens were designated as SpecimentA1, SpecimentA2, SpecimentA2, and SpecimentA3, SpecimentA4, SpecimentA5, SpecimentA6, SpecimentA7, SpecimentA8.

The eight specimens were subjected to a displacement amplitude loading pattern, AISC Modified . (Figure 4) .The AISC protocol was modified by adding three extra sets of six low amplitude cycles. Shear deformation is defined as $\gamma = \frac{\Delta}{L}$ where Δ Horizontal displacement , h-distance HBE-330 line (360mm).

The tests were performed until the complete failure of specimens.

3.1 Material Properties

Plate Material Tests

Twelve dogbone-shaped tension coupon tests were conducted on the fuse plate material. The tests took place at the Department of Structural and Geotechnical Engineering - Structure Laboratory at the University of Rome Sapienza in May, 2019. The 20 mm thick coupons were tested using the 2500kN capacity MTS machine and the 250kN capacity Ronell machine was used to test the 10 mm, 8mm and 4 mm thick coupons. UNI-EN 10002-1 and ASTM standard E8-01 was used to define the geometry of the tensile coupons. Gage lengths for instruments, types of instrumentation, speed of testing, and procedures for computing pertinent values from the data were based on UNI-EN 10002-1 and ASTM standard E8-01. The specimens were cut using a waterjet cutting machine. Specimens were cut from the same material used for the fuses. (Fig.3a, fig.3b and table). The geometry of the coupon specimens is shown in figure 4.

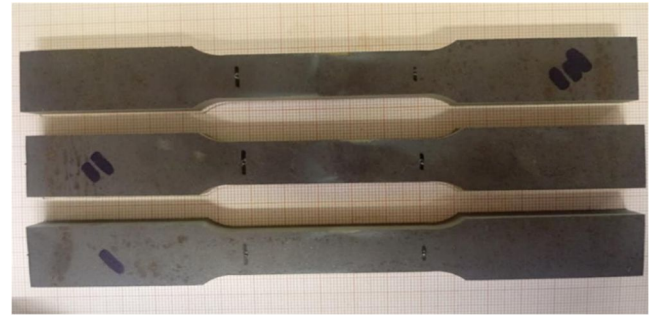


Fig.4 Geometry of the coupon

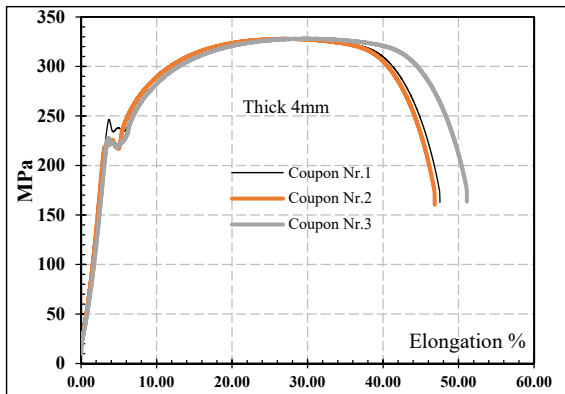


Fig.3a - Engineering stress-strain curves

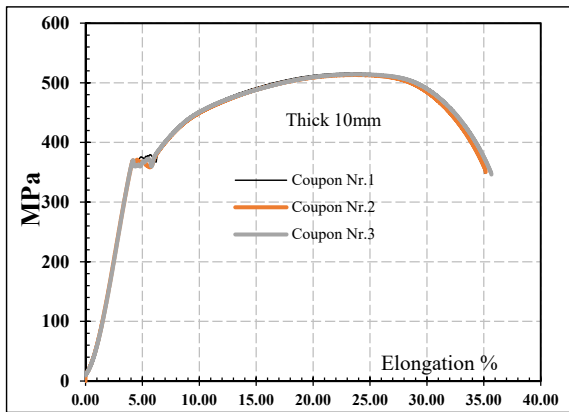


Fig.3b- Engineering stress-strain curves

Table 1 Summary of mechanical properties of plates with thickness 10 mm

Coupon	Fy (MPa)	Fu (MPa)	Elongatio n %	E
1	369,9	516,5	33,2	200 000
2	370	513,3	33,4	200 000
3	370	514,5	33,6	200 000
Averag e	369.67	514.78	33.4	200 000

3.2 Test Setup

All fuse were tested in a steel frame with a vertical actuator as shown in fig. 5 at each side the fuse, pin end structure connect the loading beam to the beam. Without the structures ,tension force will be smaller because the loading beam can move down without resistance , which reduces horizontale stretch in the damper.

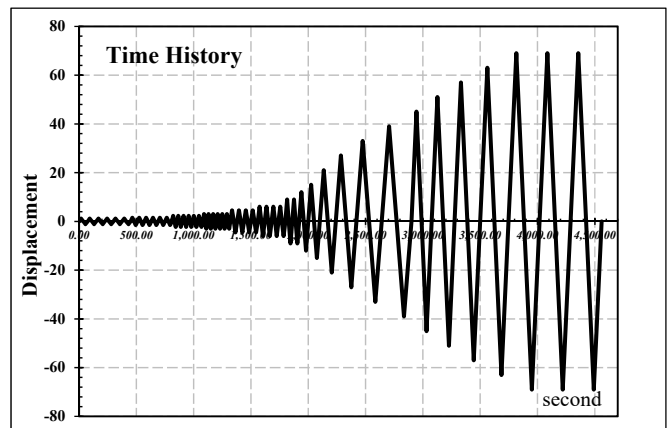
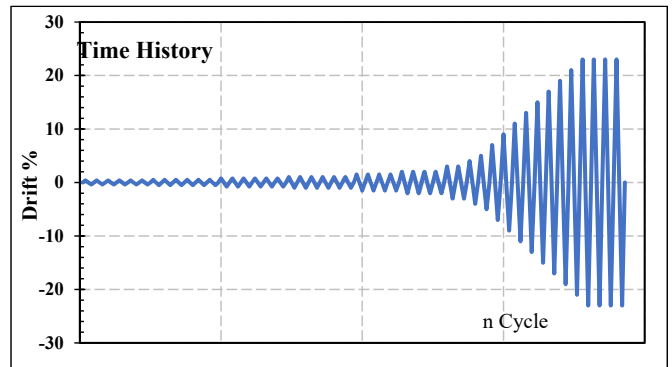


Fig 5a/5b Time history-AISC Protocol

4.0 Test Results

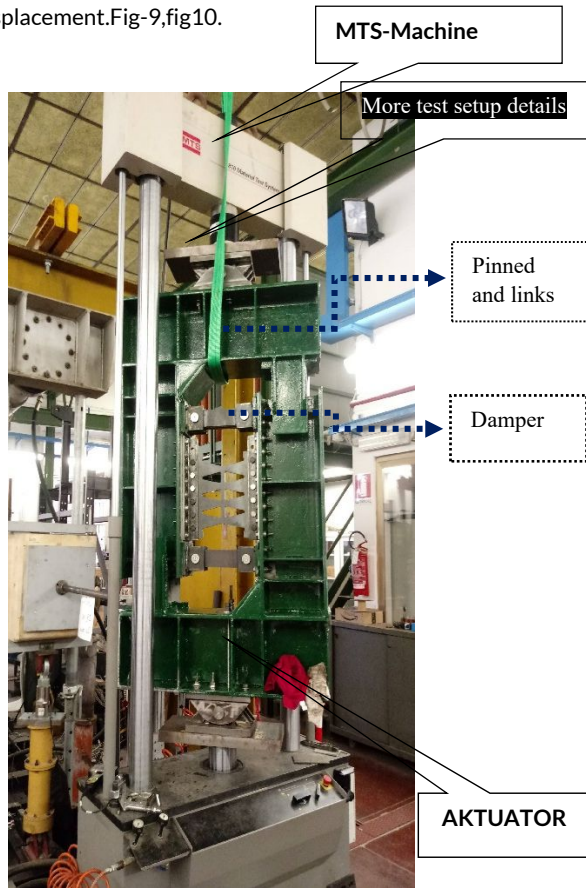
4.1) Specimen A1-4mm :

Figure shows the load deformation relationships, and illustrates the progression of deformation . Buckling started at a drift of 1.5% or 4 mm displacement. Cracks appeared at middle height section at 23% fractured in the next 4

cycle at 23% or 69mm displacement. Fig-7, fig-8.

4.2) Specimen A2-4mm

One of the objectives of this test is to study the impact of the fuse ratio on the global turn of plate shear and buckling, Fig.9 During this test, started deflecting out-of-plane at 1% or 3 mm displacement. Buckling became visible from the next drift 2% or 6 mm displacement. Crack initiated when the fuse was at the negative peak of the same cycle The fracture was not achieved even with 23% drift and after 3 cycles of 23% or 69 mm Displacement. Fig-9, fig10.



a)

Fig.6: a) Setup detail (Photo), b) Schematic

4.3) Specimen A3-8mm

This specimen differs from Specimen A3-8mm in that L/t . Load deformation relationship and fuse deformation is shown in the figure. Stable hysteretic behaviour, buckling did not appear until 7% Drift or 27mm displacement. Cracks appeared in the 17% drift, and first cycles later fractured at the middle sections at 19% Drift. Fig11, 12

4.4) Specimen A4-8mm

This specimen differs from Specimen A4-8mm in that L/t . Load deformation relationship and fuse deformation is shown in the figure. Stable hysteretic behaviour. Cracks appeared in the 5% drift, and first cycles later fractured at the top sections at 7% drift or 21 mm displacement. Fig.13, Fig-14.

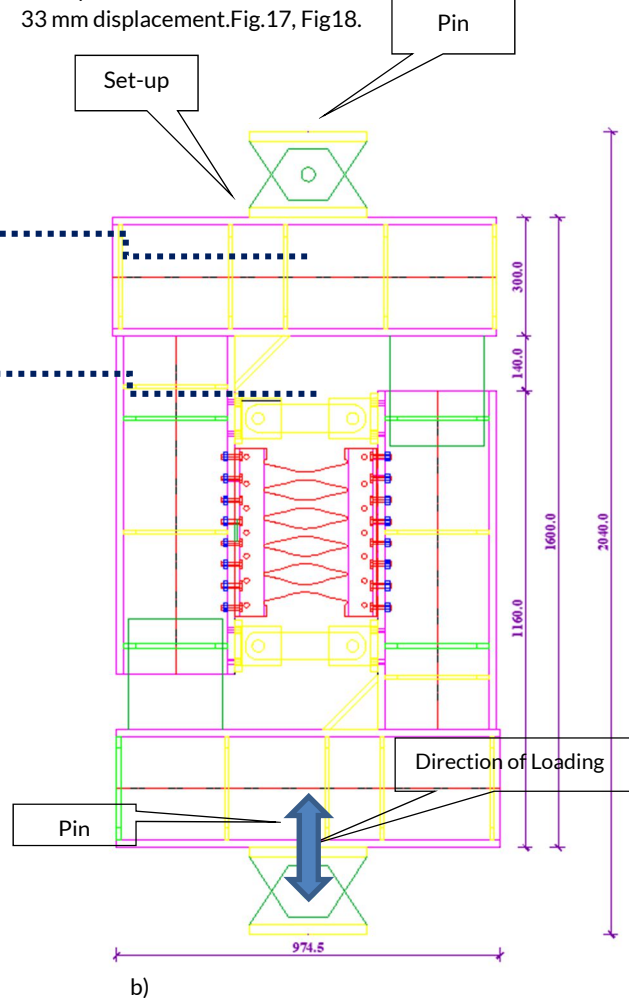
4.5) Specimen A5-10mm

This specimen differs from Specimen A4-8mm in that L/t . The load-deformation relationship and fuse deformation is shown in the

figure. Stable hysteretic behavior and increased plastic behavior. buckling did not appear until 13% Drift or 27mm displacement. Cracks appeared in the 23% drift, and first cycles later fractured at the middle sections at 23% drift or 69 mm displacement. Fig-15,16.

4.6) Specimen A6-10mm

This specimen differs from Specimen A4-8mm in that $L/t=20$. The load-deformation relationship and fuse deformation is shown in the figure. Stable hysteretic behavior and increased plastic behavior. buckling not appear. Cracks appeared in the 9% drift, and first cycles later fractured at the middle sections at 11% drift or 33 mm displacement. Fig.17, Fig18.



b)

4.7) Specimen A7-20mm

This specimen differs from Specimen A4-8mm in that L/t . Their design used b/t , and $L/T = 200/20 = 10$. Figure.. shows the load-deformation relationship which illustrates very stable hysteretic behavior in the test. No notable buckling was observed, dominated the whole test. crack initiated at a point near the middle at 23% ultimate cycle or 69 mm displacement. thick butterfly are more desirable for the purpose of energy dissipation. Fig-19, Fig-20.

4.8) Specimen A8-20mm

This specimen differs from Specimen A4-8mm in that L/t . Their design used b/t , and $L/T = 200/20 = 10$. Figure.. shows the load-deformation relationship which illustrates stable hysteretic behaviour in the test. No notable buckling was observed,

dominated the whole test. Cracks appeared in the 15% drift, and first cycles later fractured at the middle sections at 17% drift ore 51 mm displacement.Fig-21, Fig-22.

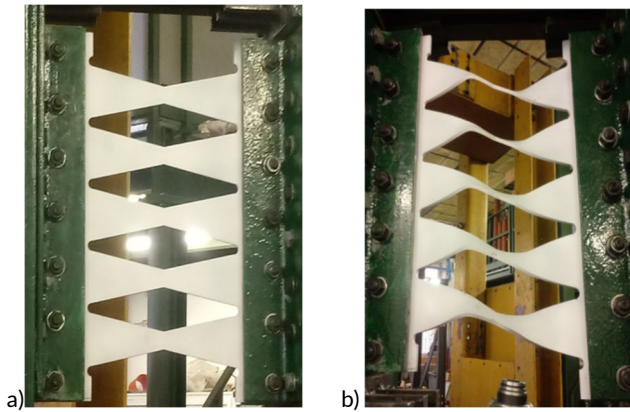


Fig.7 . Photo of Specimens A1: a)Start of the test,b) Fracture-end test

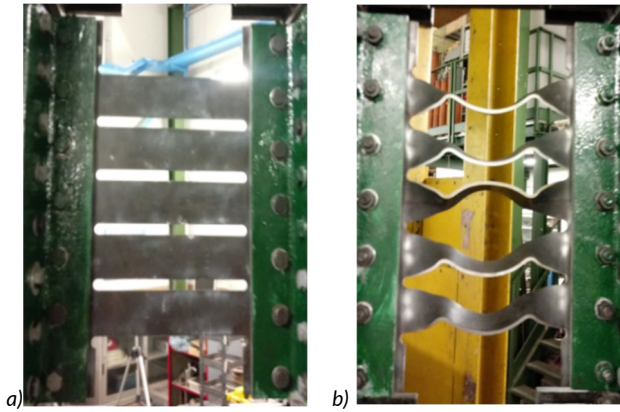


Fig.9 . Photo of Specimens A2: a)Start of the test,b) Fracture-end test

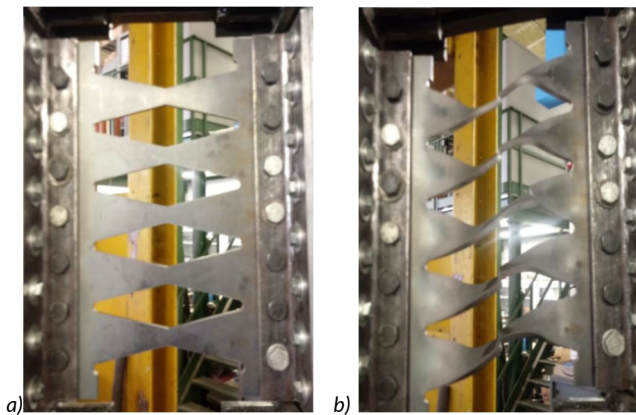


Fig.11 . Photo of Specimens A3: a)Start of the test,b) Fracture-end test

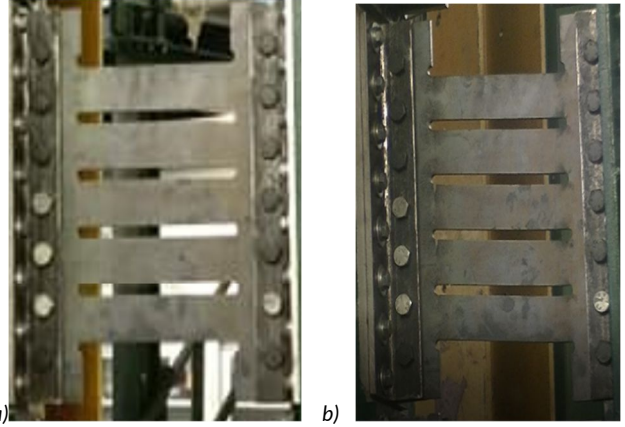


Fig.13 . Photo of Specimens A4: a)Start of the test,b) Fracture-end test

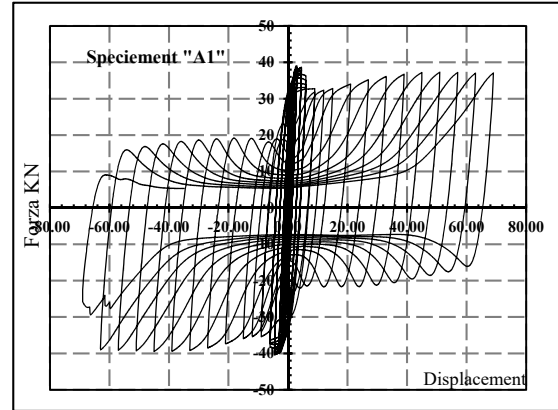


Fig.8 . Force-displacement hysteresis(SpecimenA1-4mm

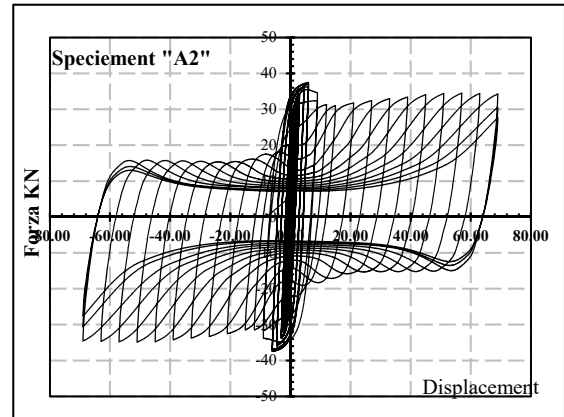


Fig.10. Force-displacement hysteresis(SpecimenA2-4mm

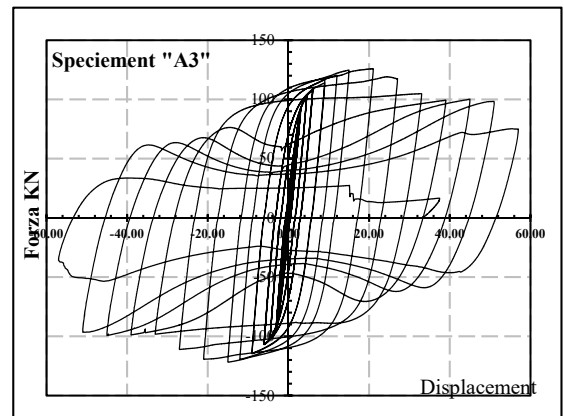


Fig.12 . Force-displacement hysteresis(SpecimenA3-8mm

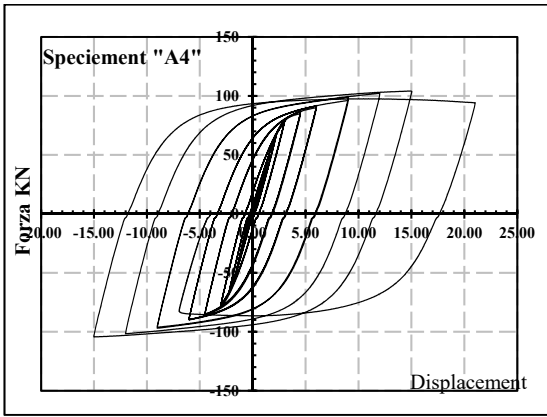


Fig.14 . Force-displacement hysteresis(SpecimenA4-8mm

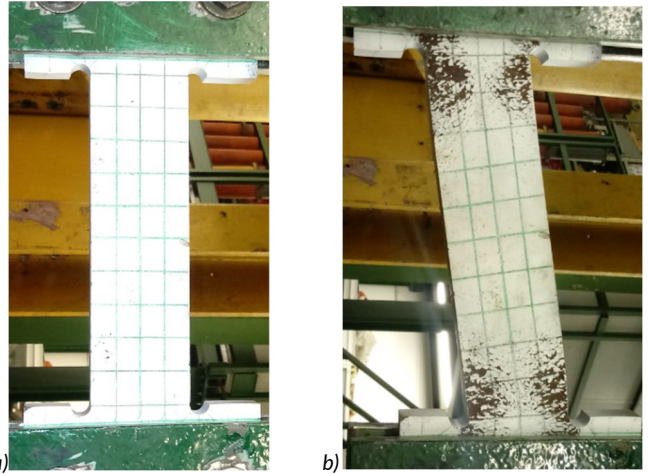


Fig.21 . Photo of Specimens A7: a)Start of the test,b) Fracture-end test

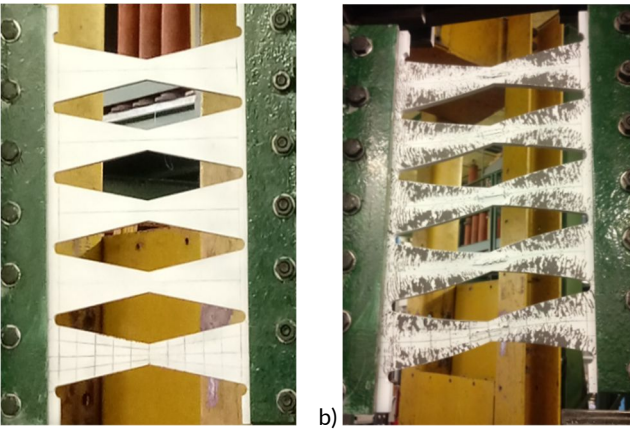


Fig.15 . Photo of Specimens A5: a)Start of the test,b) Fracture-end test

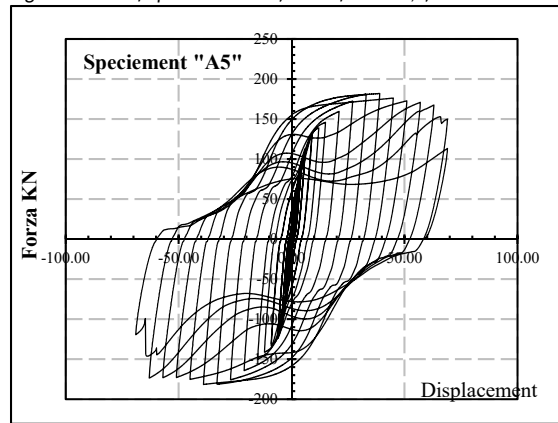


Fig.16 . Force-displacement hysteresis(SpecimenA5-10mm

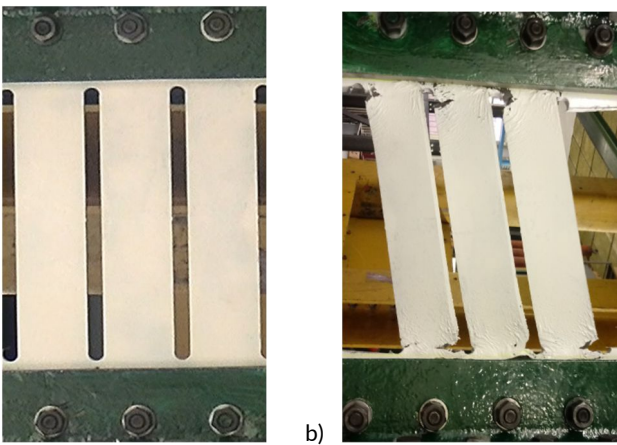


Fig.17 . Photo of Specimens A6: a)Start of the test,b) Fracture-end test

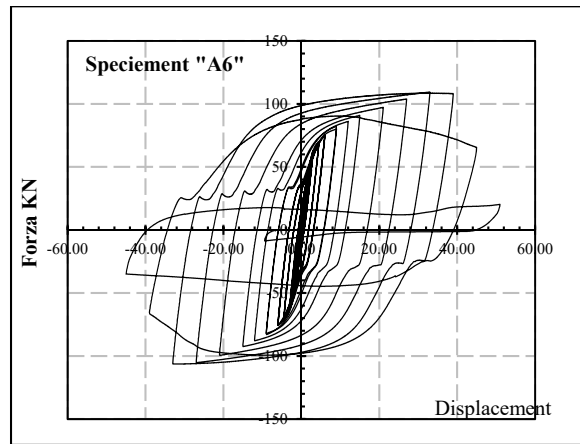


Fig.18 . Force-displacement hysteresis(SpecimenA6-10mm

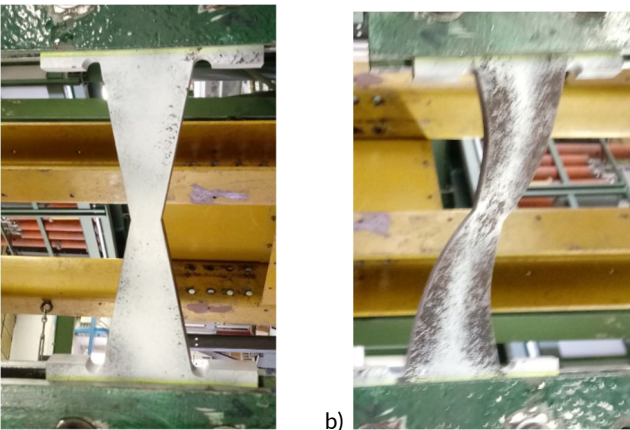


Fig.19 . Photo of Specimens A8: a)Start of the test,b) Fracture-end test

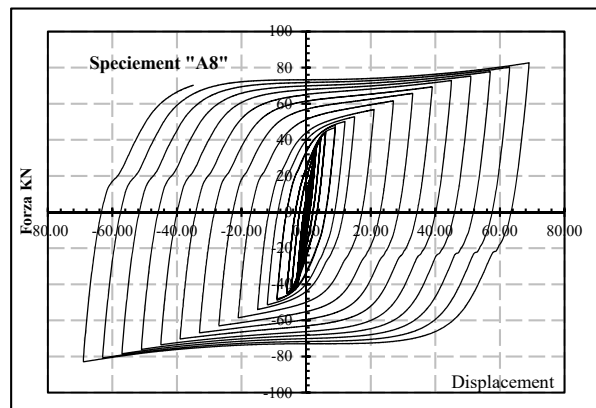


Fig.20 . Force-displacement hysteresis(SpecimenA8-20mm

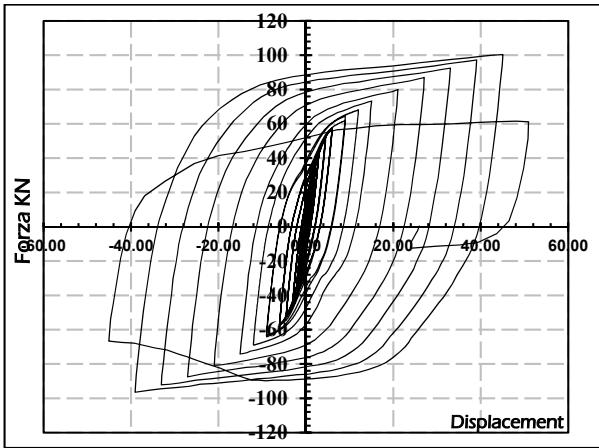


Fig.22. Force-displacement hysteresis (Specimen A7-20mm)

5.0 Energy dissipation

To investigate the effect of test parameters on the energy dissipation capacity of dampers, the slit and butterfly charts for dissipated energy were shown in Fig.23. The dissipated energy of specimens with a depth (L/t) of 10 is higher than that of specimens with a depth of 50. It can be seen from Fig.23 that as the depth ratio and the number of steel plates increase, the energy dissipation capacity increases, while there is the effect of the thickness of steel plates on energy dissipation capacity.

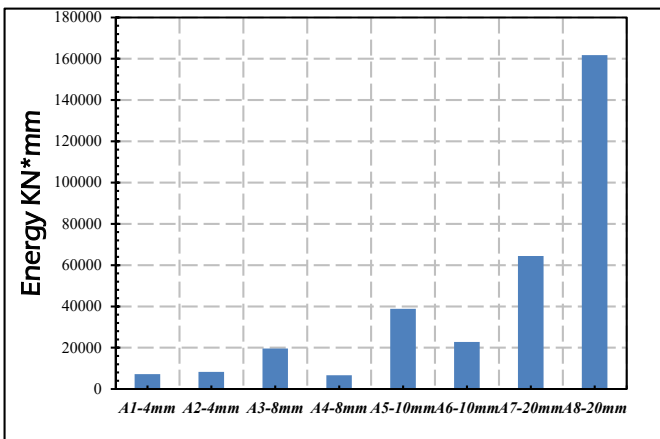


Fig.23. Dissipated Energy

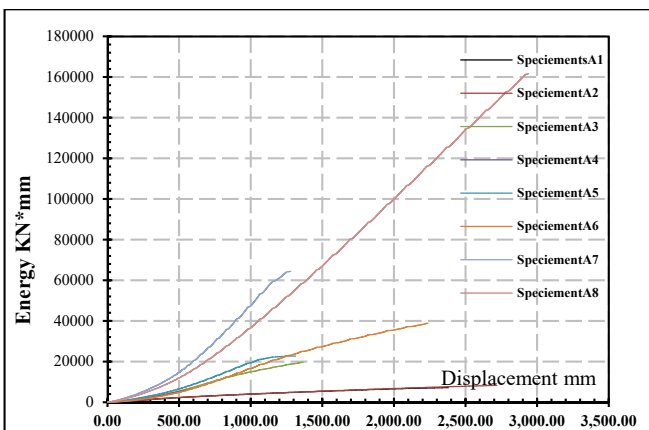


Fig.24. Dissipated Energy-Displacement

It can be seen from Fig.24 that as the depth increase, the energy dissipation capacity increases, while there is effect of the thickness

of steel plates on energy dissipation capacity.

6.0 CONCLUSIONS

This study focussed about the effect of shape variables on the performance of conventional steel slit damper. The study has been carried out for shape variables using the design of the experimental technique and the response surface method was used to study the interactions between the chosen parameters and the final response. The following conclusions are made from this study:

1. Damper configuration with increased depth of the strip has high stiffness and provides stable hysteretic curve under large displacement irrespective of strip width at mid-height.
2. Reducing the strip width at the mid-height has a high influence on the damper performance by avoiding brittle damage at the end from stress concentration.
3. Based on the response surface methodology, effective stiffness and effective damping is expressed as a function of strip width at mid-height (bc), the height of the strip (h) and thickness of the damper (t).

Acknowledgements

The authors would like to thank prof. Dr. Franco Bontempi from the "La Sapienza" University of Rome. In addition, the authors wish to acknowledge the technical staff at the Structural Testing Laboratory at the Sapienza University of Rome.

References:

- [1] Abaqus (2014). Abaqus analysis user's manual, version 16.4
- [2] Aiken, I., Nims, D., Whittaker, A., and Kelly, J. (1993). "Testing of passive energy dissipation systems"
- [3] Kobori, T., Miura, Y., Fukusawa, E., Yamada, T., Arita, T., and Takenake, Y. (1992). "Development and application of hysteresis steel dampers" Proc. 11th World Conference on Earthquake Engineering.
- [4] Amadeo, B., Sang-Hoon, O.H., Akiyama, H. (1998) "Ultimate energy absorption capacity of slit type steel plates subjected to shear deformations"
- [5] ASCE. (2010). "Minimum design loads for buildings and other structures." ASCE/SEI 7-10, ASCE, Reston, VA.
- [6] Chan, R. W. K., and Albermani, F. (2008). "Experimental study of steel slit damper for passive energy dissipation." Eng. Struct., 30(4), 1058-1066.
- [7] Dowling, N. E. (2007). Mechanical behavior of material: Engineering methods for deformation, fracture, and fatigue, 3rd Ed., Prentice Hall, NJ.
- [8] Fatemi, A., and Vang, L. (1998). "Cumulative fatigue damage and life prediction theories: A survey of the state of the art for homogeneous materials." Int. J. Fatigue, 20(1), 9-34.

- [9] FEMA. (2000). "Prestandard and commentary for the seismic rehabilitation of buildings." Rep. No. FEMA-356, FEMA, Washington, DC.
- [10] FEMA. (2007). "Interim testing protocol for determining the seismic performance characteristics of structural and nonstructural components." Rep. No. FEMA-461, FEMA, Washington, DC.
- [11] Ju, Y. K., Kim, M. H., Kim, J., and Kim, S. D. (2009). "Component tests of buckling-restrained braces with unconstrained length." *Eng. Struct.*, 31(2), 507-516.
- [12] Kim, Y. J., Jung, I. Y., Ju, Y. K., Park, S. J., and Kim, S. D. (2010). "Cyclic behavior of diagrid nodes with H-section braces." *J. Struct. Eng.*, 136(9), 1111-1122.
- [13] Krawinkler, H., and Zohrei, M. (1983). "Cumulative damage in steel structures subjected to earthquake ground motions." *Comput. Struct.*, 16(1-4), 531-541.
- [14] Miner, M. A. (1945). "Cumulative damage in fatigue." *J. Appl. Mech.*, 12(3), 159-164
- [15] Mackenzie, A. C., Hancock, J.W. & Brown, D. K. (1977), 'On the influence of state of stress on ductile failure initiation in high strength steels', *Engineering Fracture Mechanics* 9(1), 167-188.
- [16] Kanvinde, A. M. & Deierlein, G. G. (2006), 'The void growth model and the stress modified critical strain model to predict ductile fracture in structural steels', *Journal of Structural Engineering* 132(12), 1907-1918
- [17] Skinner, R. I., Kelly, J. M. & Heine, A. J. (1975), 'Hysteretic dampers for earthquake-resistant structures', *Earthquake Engineering & Structural Dynamics*
- [18] Oh, S. H., Kim, Y.-J., and Ryu, H.-S. (2009). "Seismic performance of steel structures with slit dampers." *Eng. Struct.*
- [19] Christopoulos C, Montgomery M. Viscoelastic coupling dampers (VCDs) for enhanced wind and seismic performance of high-rise buildings. *Earthq Eng Struct Dyn* 2013
- [20] Chopra, A. K. (2019): *Dynamic of structures*. Pearson Education, 5th edition, United States.
- [21] Bruneau M., Uang C.M. and Sabelli R., *Ductile design of steel structures*, McGraw Hill, Inc, 2011.